



## ORIGINAL ARTICLE

Y. Simon  
A. Marchadier  
M. K. Riviere  
K. Vandamme  
F. Koenig  
F. Lezot  
A. Trouve  
C. L. Benhamou  
J. L. Saffar  
A. Berdal  
J. R. Nefussi

**Authors' affiliations:**

Y. Simon, F. Lezot, A. Berdal, J. R. Nefussi, Team 5, UMRS 872 INSERM, Paris, France  
Y. Simon, A. Marchadier, F. Koenig, C. L. Benhamou, INSERM, U 658-IPROS CHR Orléans BP 2439, Orléans Cedex 1, France  
Y. Simon, J. L. Saffar, Dental School, University Paris 5 Descartes, Paris, France  
M. K. Riviere, INSERM, U872, Centre de recherche des Cordeliers, Université Paris 5, Université Paris 6, Paris, France  
K. Vandamme, CNRS, UMR 7052 B2OA, University Paris Diderot, Paris, France  
F. Lezot, INSERM UMR957, Faculty of Medicine, Nantes University, Nantes, France  
A. Trouve, CMLA, ENS de Cachan, Cachan Cedex, France  
A. Berdal, J. R. Nefussi, Dental School, University Paris 7 Diderot, Paris, France  
A. Berdal, J. R. Nefussi, Service d'Odontologie, AP-HP Hopital Rotchschild, Paris, France

**Correspondence to:**

Y. Simon  
Team 5  
UMRS 872 INSERM  
15 rue de l'école de médecine, 75006  
Paris, France  
E-mail: yohann.simon@free.fr

**Date:**

Accepted 17 November 2013

DOI: 10.1111/ocr.12035

© 2014 John Wiley & Sons A/S.  
Published by John Wiley & Sons Ltd

## Cephalometric assessment of craniofacial dysmorphologies in relation with *Msx2* mutations in mouse

Simon Y., Marchadier A., Riviere M. K., Vandamme K., Koenig F., Lezot F., Trouve A., Benhamou C. L., Saffar J. L., Berdal A., Nefussi J. R. Cephalometric assessment of craniofacial dysmorphologies in relation with *Msx2* mutations in mouse  
*Orthod Craniofac Res* 2014; **17**: 92–105. © 2014 John Wiley & Sons A/S. Published by John Wiley & Sons Ltd

**Structured Abstract**

**Objectives** – To determine the role of *Msx2* in craniofacial morphology and growth, we used a mouse model and performed a quantitative morphological characterization of the *Msx2*<sup>-/-</sup> and the *Msx2*<sup>+/-</sup> phenotype using a 2D cephalometric analysis applied on micrographs.

**Materials and Methods** – Forty-four three-and-a-half-month-old female CD1 mice were divided into the following three groups: *Msx2*<sup>+/+</sup> (n = 16), *Msx2*<sup>+/-</sup> (n = 16), and *Msx2*<sup>-/-</sup> (n = 12). Profile radiographs were scanned. Modified cephalometric analysis was performed to compare the three groups.

**Results** – Compared with the wild-type mice, the *Msx2*<sup>-/-</sup> mutant mice presented an overall craniofacial size decrease and modifications of the shape of the different parts of the craniofacial skeleton, namely the neurocranium, the viscerocranium, the mandible, and the teeth. In particular, dysmorphologies were seen in the cochlear apparatus and the teeth (taurodontism, reduced incisor curvature). Finally contrary to previous published results, we were able to record a specific phenotype of the *Msx2*<sup>+/-</sup> mice with this methodology. This *Msx2*<sup>+/-</sup> mouse phenotype was not intermediate between the *Msx2*<sup>-/-</sup> and the wild-type animals.

**Conclusion** – *Msx2* plays an important role in craniofacial morphogenesis and growth because almost all craniofacial structures were affected in

the *Msx2*<sup>-/-</sup> mice including both intramembranous and endochondral bones, the cochlear apparatus, and the teeth. In addition, *Msx2* haploinsufficiency involves a specific phenotype with subtle craniofacial structures modifications compared with human mutations.

**Key words:** 2D cephalometric analysis; animal model; craniofacial morphology; microradiograph; *Msx2*

## Introduction

Craniofacial morphogenesis and growth depend on developmental genes encoding a variety of transcription factors, growth factors, and receptors (1, 2). Among these are members of the Muscle segment homeobox gene family (*Msx*). *Msx1* and *Msx2* (two of the three physically unlinked members of the *Msx* gene family) are strongly expressed in developing craniofacial regions, and their spatial and temporal expression correlates with crucial aspects of craniofacial morphogenesis (3–5).

In humans, *MSX2* mutations provoke defects in craniofacial sutures (6). *MSX2* loss-of-function mutation causes enlarged parietal foramina (7), while *MSX2* gain-of-function mutation results in premature ossification of the calvaria suture (Boston type craniosynostosis) and abnormal skull shape (6). All aforementioned studies underline the pivotal role of *MSX2* in the development and morphology of the craniofacial bone structures.

*Msx2*-deficient mice display a wide spectrum of dysmorphologies involving not only the skeleton of the skull but also tooth morphology and eruption as well as periodontal defects (4, 8, 9). Thus *Msx2* seems to play a crucial role in craniofacial and teeth morphology.

The genetic etiology of craniofacial growth is poorly known. The goal of the present study is to better understand the role of *Msx2* gene on the different parts of the craniofacial morphology and to find new morphologic signs which could be symptomatic of *Msx2* mutations. Most of the craniofacial bones and teeth dysmorphologies related to *Msx2* mutations were recorded by whole mount procedures and by histology sections (8, 9). However, quantitative data and the effective action on the different craniofacial structures are lacking. Therefore, we propose to describe quantitatively the craniofa-

cial bone and teeth dysmorphologies related to *Msx2* loss-of-function mutation using a cephalometric analysis on lateral radiographs following Engstrom et al. (10). To this end, we compared the different craniofacial regions of the homozygous *Msx2*<sup>-/-</sup> and the heterozygous *Msx2*<sup>+/-</sup> mutant mice to the wild-type mice.

## Materials and methods

### Experimental animals

All experiments were performed in accordance with the French National Consultative Bioethics Committee for Health and Life science, following ethical guidelines for animal care.

Forty-four three-and-a-half-month-old female CD-1 Swiss mice were used and were divided into the following three genotypic groups: *Msx2*<sup>+/+</sup> (n = 16), *Msx2*<sup>+/-</sup> (n = 16), and *Msx2*<sup>-/-</sup> (n = 12) mice. The *Msx2* mutant mice were generated through gene knock-in, with the *Msx2* gene replaced by the bacterial nLacZ gene (11). This targeted insertion involves a complete suppression of the *Msx2* gene and evokes a loss-of-function mutation. The *Msx2* mutant mice initially made on a C57/BL6 background had been backcrossed for at least ten generations onto the CD1 Swiss genetic background for these experiments. Animals were sacrificed after inhalation anesthesia.

### Morphological measurements

A microfocal X-Ray machine was used (Tubix sigma 2060, Paris, France) at a focal distance of 56 mm under an electric condition of 12 mA and 13 kV with an exposure time of 15 min. High-resolution films SO-343 (KODAK Professional; 10.2 × 12.7 cm; Eastman Kodak Company, New York, NY, USA) were used. Object magnification was minimized through direct

positioning of the object onto the film. The microradiographs were scanned (EPSON Perfection 1640–3200 dpi digital resolution) and were subsequently reoriented to achieve a horizontal alignment of the occipito-interparietal suture and the nasal bone extremity (Rhinion).

Cephalometric analysis was performed according to a method described by Engstrom et al. (10). Thirty-one anatomical landmarks and two constructed points (T and K) (12) were defined for this study allowing 46 measurement items as depicted in Fig. 1. The distance Mn-T determines the depth of the antegonial notch curvature, and the distance GnK determines the height of the angular process.

The scanned images of the craniofacial area were analyzed using ImageJ (Rasband, WS, ImageJ; US National Institutes of Health, Bethesda, MD, USA, <http://rsbweb.nih.gov/ij/>, 1997–2012).

#### Statistical analysis

Nonparametric Kruskal–Wallis tests were used to determine whether there was a significant difference in measured values between the three groups (*Msx2*<sup>-/-</sup>, *Msx2*<sup>+/-</sup>, and *Msx2*<sup>+/+</sup>) after performing Levene’s tests. Indeed, Levene’s tests were significant for some variables, meaning that homogeneity of variances across groups could not be ensured and therefore one-way analysis of variance (ANOVA) could not be performed. To take into account testing multiple variables, *p*-values were adjusted to control the false discovery rate (FDR) to a 5% level. Mann–Whitney Wilcoxon tests were used as *post hoc* test to compare groups in pairs when Kruskal–Wallis test was significant. *p*-Values were adjusted using Bonferroni correction to consider multiple comparisons between groups. The statistical analysis was performed using R software version 2.15 (13).

#### Method error

All different points were located in quadruplicate on nine different microradiographs randomly chosen, in a non-consecutive manner (one series per day).

*I* landmarks (noted *i*) (*I* = 31), *H* the subjects (noted *h*) (*H* = 9), *K* the number of recording for

each subject (*K* = 4), *L* the number of coordinates (*L* = 2 in *R*<sup>2</sup>). The mean standard deviation reproducibility error estimate for landmark *i* can be computed by:

$$\sigma_{i,\text{rep}} = \left( \frac{1}{h(K-1)L} \sum_{h=1}^H \sum_{k=1}^K \sum_{l=1}^L \left( Z_{ihk}^{(l)} - \bar{Z}_{ih}^{(l)} \right)^2 \right)^{\frac{1}{2}}$$

$Z_{ihk}^{(l)}$  is the *l* coordinate of landmark *i* of the subject *h* computed at the *k* recording.

$$\bar{Z}_{ih}^{(l)} = \frac{1}{K} \sum_{k=1}^K Z_{ihk}^{(l)}$$

A mean standard deviation on all the landmarks estimate is:

$$\sigma_{\text{rep}} = \left( \frac{1}{I} \sum_{i=1}^I \sigma_{i,\text{rep}}^2 \right)^{\frac{1}{2}}$$

The mean standard deviation on all the landmarks was 117 μm which revealed to be significantly lower than the computed cephalometric differences between the three groups.

## Results

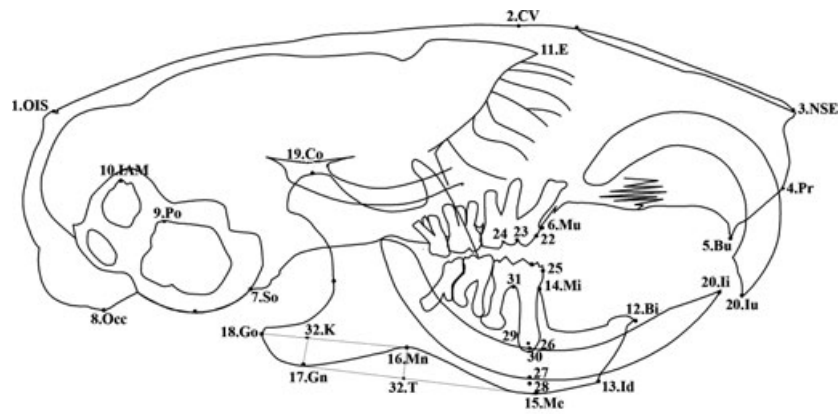
Forty-six measurement items were used for the cephalometric analysis and expressed as means and standard deviations for linear and angular measurements for the three genotypic groups (Figs 2–10). The results are presented in Table 1.

#### Total skull

The *Msx2*<sup>-/-</sup> mice skull size [perimeter, length (OIS–NSE; Occ–Pr), and height (CV–Gn)] was significantly smaller than in the *Msx2*<sup>+/-</sup> and wild-type mice (*p* < 0.05 for all parameters) (Fig. 3). However, no significant difference was observed between the *Msx2*<sup>+/-</sup> and the wild-type mice.

#### Neurocranium

The posterior neurocranium height (OIS–Occ) and the size of the anterior cranial base (So–E) were significantly reduced in the *Msx2*<sup>-/-</sup> mice



31 points have been chosen to characterize the dimensions and the shape of the head.

1. O.I.S. : occipito-interparietal suture	2. C.V. :cranial vertex
3. Rhinion: Nasale Spine Extremity (NSE): the most anterior point of the nasal bone	4. Pr: the most anterior and lower point of the vestibular alveolar process of the incisal bone (premaxilla).
5. Bu: the most anterior and lower point of the lingual alveolar process of the incisal bone (premaxilla).	6. Mu : the lowest point of the mesial alveolar process of upper M1
7. So:Intersection between the tympanic bulla and the posterior border of the basisphenoid	8. Occ:The lowest point of the occipital condyle.
9. Po: porion: highest point of the external acoustic meatus.	10. IAM: Highest point of the internal acoustic meatus.
11. E:Intersection between frontal bone and most supero-anterior point of the posterior limit to the ethmoid bone	12. BI: the most anterior point of the lingual mandibular alveolar ridge
13. Id: the most anterior point of the vestibular mandibular alveolar process	14. MI: the highest point of the mesial alveolar process of the lower first molar.
15. Me : lowest point of the mandibular corpus	16. Mn : A point in the deepest part of the antegonial notch curvature
17. Gn : lowest point of the ramus, or of the angular process	18. Go: point the most posterior of the gonial angle or of the angular process
19. Co: point the highest of the condyle	20. Iu. : upper incisor edge
21. li. : lower incisor edge	22. center of the anterior face of the first upper molar crown.
23. U1: A point on the mesial occlusal fossa of the upper first molar	24. U2: A point on the distal occlusal fossa of the upper second molar
25. center of the anterior face of the first lower molar crown.	26. the most inferior point of the lingual face of the lower incisor
27. the lowest point of the vestibular face of the lower incisor	28. the lowest point of the vestibular periodontal ligament
29. the highest point of the lingual periodontal ligament with the same abscissa than the point 28	30. M1 mesial root apical foramina
31. M1 furcation	

Fig. 1. Thirty-one points have been chosen to characterize the dimensions and the shape of the head.

compared with the *Msx2*<sup>+/-</sup> and to the wild-type mice ( $p < 0.001$  and  $p < 0.005$ , respectively) (Fig. 4). Occ-OIS/So-E was significantly increased in the *Msx2*<sup>-/-</sup> mice compared with the two other groups ( $p < 0.005$  and  $p < 0.05$ , respectively), showing modifications of the shape of the neurocranium.

#### Upper viscerocranium

Compared with the *Msx2*<sup>+/-</sup> and with the wild-type mice, the *Msx2*<sup>-/-</sup> mice had a larger anterior facial height (NSE-Pr;  $p < 0.001$  and  $p < 0.0001$ , respectively). This measure was also more important for the *Msx2*<sup>+/-</sup> mice than for the wild animal ( $p < 0.05$ ). Furthermore, compared with the *Msx2*<sup>+/-</sup> and the wild type, the *Msx2*<sup>-/-</sup> mice

exhibited a reduced size of the emerging upper incisor (Pr-Iu;  $p < 0.01$  and  $p < 0.005$ , respectively) and a smaller palatal length (Mu-Bu;  $p < 0.0005$  and  $p < 0.01$ , respectively).

Concerning the angular parameters, the *Msx2*<sup>-/-</sup> mice, compared with the *Msx2*<sup>+/-</sup> and the wild-type mice, had a retrognathic position of the maxilla related to the cranial vault reference (E-Pr/E-OIS was significantly reduced;  $p < 0.0001$  and  $p < 0.001$ , respectively) as well as related to the anterior cranial base (E-Pr/E-So was significantly smaller;  $p < 0.005$ ).

#### Mandible

Compared with the *Msx2*<sup>+/+</sup> mice, the *Msx2*<sup>-/-</sup> mice exhibited a smaller mandibular corpus

**Table 1. Craniofacial cephalometric analyses (mean ± SD) in *Msx2*<sup>-/-</sup>, *Msx2*<sup>+/-</sup> and *Msx2*<sup>+/+</sup> mice**

Variable	Mean (standard deviation)			Kruskal–Wallis test difference between all three groups	Mann–Whitney Wilcoxon test		
	<i>Msx2</i> <sup>-/-</sup>	<i>Msx2</i> <sup>+/-</sup>	<i>Msx2</i> <sup>+/+</sup>		<i>Msx2</i> <sup>-/-</sup> vs. <i>Msx2</i> <sup>+/-</sup> p-Value	<i>Msx2</i> <sup>-/-</sup> vs. <i>Msx2</i> <sup>+/+</sup> p-Value	<i>Msx2</i> <sup>+/-</sup> vs. <i>Msx2</i> <sup>+/+</sup> p-Value
<b>Total skull</b>							
Cranio-facial perimeter	62.65 (±2.37)	65.80 (±1.42)	67.10 (±2.53)	<b>0.0003</b>	<b>0.0023</b>	<b>0.0003</b>	0.4403
Skull length							
OIS-NSE	22.23 (±0.84)	23.21 (±0.42)	23.05 (±0.51)	<b>0.0147</b>	<b>0.0299</b>	<b>0.0342</b>	1.0000
Occ-Pr	22.22 (±0.98)	23.94 (±0.48)	23.74 (±0.35)	<b>0.0002</b>	<b>0.0002</b>	<b>0.0014</b>	0.3807
Skull height							
CV-Mn	10.04 (±0.27)	10.28 (±0.32)	10.41 (±0.52)	<b>0.0405</b>	0.0647	0.0823	1.0000
CV-Gn	10.82 (±0.35)	11.75 (±0.61)	12.05 (±0.79)	<b>0.0006</b>	<b>0.0019</b>	<b>0.0011</b>	0.9000
<b>Neurocranium</b>							
<i>Linear values</i>							
Neurocranium length: OIS-E	14.44 (±0.41)	14.45 (±0.43)	14.63 (±0.36)	0.3180			
Neurocranium height: OIS-Occ	5.46 (±0.36)	6.77 (±0.14)	6.62 (±0.20)	<b>0.0000</b>	<b>0.0000</b>	<b>0.0000</b>	0.0711
Posterior skull basis length: Occ-So	5.32 (±0.23)	5.39 (±0.32)	5.28 (±0.15)	0.2097			
Anterior skull basis length: So-E	10.12 (±0.55)	10.93 (±0.79)	10.7 (±0.57)	<b>0.0003</b>	<b>0.0023</b>	<b>0.0008</b>	0.2804
<i>Angular values</i>							
Cranial vault: OIS-CV/CV-Na	19.39 (±3.06)	13.73 (±2.36)	12.46 (±1.79)	<b>0.0000</b>	<b>0.0000</b>	<b>0.0000</b>	0.6202
Between skull vault and skull base: E-OIS/E-So	30.64 (±1.81)	31.64 (±3.12)	33.25 (±2.64)	<b>0.0025</b>	<b>0.0044</b>	<b>0.0051</b>	1.0000
Occ-OIS/So-E	65.15 (±3.95)	60.18 (±1.74)	61.44 (±3.32)	<b>0.0033</b>	<b>0.0011</b>	<b>0.0442</b>	1.0000
Occ-OIS/Occ-So	92.61 (±5.40)	81.79 (±3.55)	87.56 (±4.74)	<b>0.0001</b>	<b>0.0001</b>	0.0821	<b>0.0029</b>
OIS-Occ/OIS-E	84.03 (±3.29)	86.91 (±1.55)	85.46 (±2.31)	<b>0.0277</b>	<b>0.0390</b>	0.8251	0.1567
Skull base angle: So-Occ/So-E	152.54 (±3.18)	158.39 (±4.16)	154.21 (±4.17)	<b>0.0040</b>	<b>0.0052</b>	1.0000	<b>0.0264</b>
<b>Upper viscerocranium</b>							
<i>Linear values</i>							
Anterior facial height: NSE-Pr	3.43 (±0.68)	2.50 (±0.34)	2.28 (±0.22)	<b>0.0000</b>	<b>0.0007</b>	<b>0.0001</b>	<b>0.0189</b>

**Table 1. (continued)**

Variable	Mean (standard deviation)			Kruskal–Wallis test difference between all three groups	Mann–Whitney Wilcoxon test		
	<i>Msx2</i> <sup>-/-</sup>	<i>Msx2</i> <sup>+/-</sup>	<i>Msx2</i> <sup>+/+</sup>		<i>Msx2</i> <sup>-/-</sup> vs. <i>Msx2</i> <sup>+/-</sup> p-Value	<i>Msx2</i> <sup>-/-</sup> vs. <i>Msx2</i> <sup>+/+</sup> p-Value	<i>Msx2</i> <sup>+/-</sup> vs. <i>Msx2</i> <sup>+/+</sup> p-Value
Central height of the viscerocranium: E-Mu	4.81 (±0.24)	5.18 (±0.23)	5.02 (±0.22)	<b>0.0033</b>	<b>0.0228</b>	0.0926	<b>0.0189</b>
Size of the emerging upper incisor: Pr-Iu	2.32 (±0.99)	3.59 (±0.35)	3.68 (±0.23)	<b>0.0018</b>	<b>0.0071</b>	<b>0.0027</b>	1.0000
Palatal length: Mu-Bu	5.39 (±0.37)	6.06 (±0.25)	5.83 (±0.15)	<b>0.0001</b>	<b>0.0003</b>	<b>0.0083</b>	<b>0.0236</b>
<i>Angular values: maxillary antero-posterior position</i>							
Maxilla position related to skull base: E-Pr/E-So	109.54 (±5.60)	117.50 (±2.76)	117.00 (±4.22)	<b>0.0012</b>	<b>0.0016</b>	<b>0.0044</b>	1.0000
Maxilla position related to skull vault: E-Pr/E-OIS	140.18 (±5.32)	149.14 (±1.68)	150.25 (±4.46)	<b>0.0001</b>	<b>0.0001</b>	<b>0.0008</b>	1.0000
Maxilla position related to skull vault: E-Bu/E-OIS	134.34 (±3.57)	138.15 (±2.25)	136.96 (±2.85)	<b>0.0033</b>	<b>0.0032</b>	0.0503	0.4402
<b>Mandible</b>							
<i>Linear values</i>							
Mandibular length: Co-Id	11.09 (±0.66)	11.30 (±0.62)	11.20 (±0.48)	0.4652			
Mandibular corpus length: Go-Id	10.34 (±0.49)	10.72 (±0.62)	10.94 (±0.34)	<b>0.0312</b>	0.2980	<b>0.0149</b>	1.0000
Anterior part of the mandibular corpus length: Mn-Id	6.38 (±0.61)	6.07 (±0.44)	0.61 (±0.43)	0.8321			
Mandibular ramus length: Co-Gn	5.74 (±0.25)	6.21 (±0.18)	5.95 (±0.27)	<b>0.0003</b>	<b>0.0003</b>	0.0731	<b>0.0211</b>
Angular process length: Go-Mn	4.10 (±0.57)	4.66 (±0.49)	4.84 (±0.25)	<b>0.0011</b>	<b>0.0262</b>	<b>0.0005</b>	0.7510

**Table 1. (continued)**

Variable	Mean (standard deviation)			Kruskal–Wallis test difference between all three groups	Mann–Whitney Wilcoxon test		
	<i>Msx2</i> <sup>-/-</sup>	<i>Msx2</i> <sup>+/-</sup>	<i>Msx2</i> <sup>+/+</sup>		<i>Msx2</i> <sup>-/-</sup> vs. <i>Msx2</i> <sup>+/-</sup> p-Value	<i>Msx2</i> <sup>-/-</sup> vs. <i>Msx2</i> <sup>+/+</sup> p-Value	<i>Msx2</i> <sup>+/-</sup> vs. <i>Msx2</i> <sup>+/+</sup> p-Value
Extra-bone part of the lower incisor: li-ld	4.33 (±0.65)	5.31 (±0.42)	5.27 (±0.18)	<b>0.0010</b>	<b>0.0032</b>	<b>0.0023</b>	0.7054
Antegonial notch depth: Mn-T	0.62 (±0.09)	1.02 (±0.72)	0.87 (±0.10)	<b>0.0001</b>	<b>0.0002</b>	<b>0.0001</b>	1.0000
<i>Angular values</i>							
Mandible position related to skull base: E-So/E-ld	69.06 (±3.94)	65.92 (±2.71)	65.30 (±3.12)	0.1206			
Antegonial notch angle: Mn-Gn/Mn-ld	168.76 (±4.72)	162.10 (±4.32)	164.28 (±4.67)	<b>0.0213</b>	<b>0.0172</b>	0.1798	0.8482
Gonial angle: Go-Co/Go-Me	92.10 (±6.97)	86.06 (±3.76)	83.56 (±3.77)	<b>0.0008</b>	<b>0.0172</b>	<b>0.0010</b>	0.2203
<b>Antero-posterior discrepancy of the skeletal base and dental arches</b>							
Linear bone base discrepancy	4.90 (±0.51)	5.98 (±0.27)	5.87 (±0.25)	<b>0.0001</b>	<b>0.0002</b>	<b>0.0004</b>	0.7267
Linear antero-posterior dental arches discrepancy: Mu abscissa-MI abscissa	0.542 (±0.23)	0.40 (±0.19)	0.34 (±0.17)	0.1511			
<b>Cochlear apparatus</b>							
Po-IAM/SOI-NBE	140.59 (±5.40)	149.28 (±4.11)	146.07 (±3.96)	<b>0.0003</b>	<b>0.0003</b>	<b>0.0082</b>	0.2026
<b>Teeth</b>							
Thickness of the vestibular periodontal ligament of the lower incisor	0.45 (±0.11)	0.12 (±0.02)	0.11 (±0.04)	<b>0.0000</b>	<b>0.0000</b>	<b>0.0000</b>	1.0000

**Table 1. (continued)**

Variable	Mean (standard deviation)			Kruskal–Wallis test difference between all three groups	Mann–Whitney Wilcoxon test		
	<i>Msx2</i> <sup>-/-</sup>	<i>Msx2</i> <sup>+/-</sup>	<i>Msx2</i> <sup>+/+</sup>		<i>Msx2</i> <sup>-/-</sup> vs. <i>Msx2</i> <sup>+/-</sup> <i>p</i> -Value	<i>Msx2</i> <sup>-/-</sup> vs. <i>Msx2</i> <sup>+/+</sup> <i>p</i> -Value	<i>Msx2</i> <sup>+/-</sup> vs. <i>Msx2</i> <sup>+/+</sup> <i>p</i> -Value
Thickness of the lingual periodontal ligament of the lower incisor	0.09 (±0.04)	0.13 (±0.04)	0.22 (±0.04)	<b>0.0000</b>	<b>0.0052</b>	<b>0.0001</b>	<b>0.0008</b>
Thickness of the lower incisor	0.86 (±0.12)	0.99 (±0.04)	1.00 (±0.05)	<b>0.0004</b>	<b>0.0006</b>	<b>0.0016</b>	0.6072
External lower incisor curvature	1.2E-03 (±1.2E-04)	1.3E-03 (±1.2E-04)	1.3E-03 (±6.9E-05)	<b>0.0137</b>	0.1449	<b>0.0100</b>	0.7238
Lower M1 height (furcation-top of the crown)	2.00 (±0.11)	2.50 (±0.1)	2.60 (±0.29)	<b>0.0001</b>	<b>0.0001</b>	<b>0.0001</b>	1.0000
Lower M1 crown height	0.71 (±0.12)	0.70 (±0.01)	0.62 (±0.04)	<b>0.0064</b>	1.0000	<b>0.0363</b>	<b>0.0081</b>
Lower M1 root height	1.30 (±0.13)	1.33 (±0.01)	1.90 (±0.14)	<b>0.0001</b>	<b>0.0001</b>	<b>0.0001</b>	0.1558
M1 mesial alveolar bone height	1.14 (±0.16)	1.57 (±0.14)	1.68 (±0.15)	<b>0.0001</b>	<b>0.0003</b>	<b>0.0003</b>	0.2384

Unit of linear values: millimeter (mm); Unit of angular values: degree (°). For abbreviations: See Fig. 1. Significant values are written in bold.

length (Go-Id) ( $p < 0.05$ ). Compared with the *Msx2*<sup>+/-</sup> mice, the *Msx2*<sup>-/-</sup> mice presented a decreased ramus length (Co-Gn) ( $p < 0.0005$ ). Compared with the wild-type mice, and with the *Msx2*<sup>+/-</sup> mice, the *Msx2*<sup>-/-</sup> mice presented a shorter angular process length (Go-Mn) ( $p < 0.0005$  and  $p < 0.05$ , respectively) and the antegonial notch depth (Mn-T) was smaller ( $p < 0.0005$  and  $p < 0.0001$  respectively).

The gonial angle (Go-Co/Go-Me) was significantly larger in the *Msx2*<sup>-/-</sup> mice compared with the heterozygous and the wild-type mice ( $p < 0.05$  and  $p < 0.001$ , respectively). The antegonial notch angle (Mn-Gn/Mn-Id) was significantly larger in the *Msx2*<sup>-/-</sup> mice compared with the heterozygous mice ( $p < 0.05$ ).

#### Evaluation of the antero-posterior relationship of the skeletal base and dental arches

The linear evaluation of the antero-posterior relationship of the skeletal bases revealed that the *Msx2*<sup>-/-</sup> mice presented a smaller bone basis discrepancy compared with the one of the *Msx2*<sup>+/-</sup> and the wild-type mice ( $p < 0.0005$  for both comparison).

#### Cochlear apparatus orientation

Compared with the wild-type mice, the cochlear apparatus orientation (Po-IAM/OIS-NSE) displayed a significant clockwise rotation in the *Msx2*<sup>-/-</sup> mice ( $p < 0.01$ ).

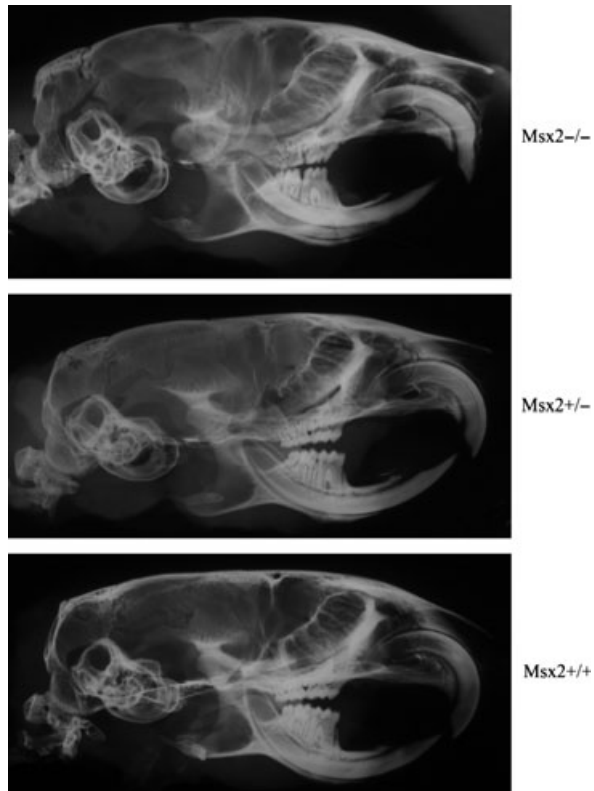


Fig. 2. Micrographs of three different genotypic mice.

### Teeth

Compared with the *Msx2*<sup>+/+</sup> and with the *Msx2*<sup>+/-</sup> mice, the extra-bone part of the lower incisor (Ii-Id) was smaller in the *Msx2*<sup>-/-</sup> mice ( $p < 0.005$  for both comparisons) (Figs 3 and 4). In addition, the buccal periodontal ligament was thicker ( $p < 0.0001$  for both comparisons), and the lingual periodontal ligament, that is, the mouse counterpart of the human periodontal ligament, was thinner ( $p < 0.001$  and  $p < 0.0001$ , respectively). Furthermore, the lower incisor was thinner ( $p < 0.001$  and  $p < 0.001$ ).

The internal and external curvatures of the upper and lower incisors were significantly reduced in the *Msx2*<sup>-/-</sup> mice compared with the wild-type mice. The lower first molar of the *Msx2*<sup>-/-</sup> mice was significantly smaller compared with the heterozygous ( $p < 0.0001$ ) and the wild-type mice ( $p < 0.0001$ ); this difference was mainly due to a reduced root height ( $p < 0.0001$  for both comparisons). The anatomical crown height (distance between the top of the crown and the furcation) was increased in the *Msx2*<sup>-/-</sup> and the *Msx2*<sup>+/-</sup> mice compared with the wild-

type mice ( $p < 0.001$  and  $p < 0.05$ , respectively). The alveolar bone height at the mesial side of the lower first molar was significantly reduced in the *Msx2*<sup>-/-</sup> mutant mice compared with the other groups ( $p < 0.0005$  for both comparisons).

## Discussion

### *Msx2* in craniofacial growth

The cephalometric analysis used in this study allowed a quantification of the dysmorphologies related to *Msx2* mutation and therefore underlined the role of *Msx2* on the different aspects of craniofacial growth. Indeed, *Msx2* null mutant mice exhibited a decrease in the craniofacial length (OIS-NSE, Occ-Pr) and height (CV-Mn, CV-Gn). As this reduction was not isometric (*i.e.*, not the same in the different spatial directions), the *Msx2*<sup>-/-</sup> mice presented a global modified skull shape. Satokata et al. (8) reported a generalized decrease in the axial and appendicular skeletal lengths. The femur and the tibia lengths were reduced to 83 and 88%, respectively, compared with the wild type. These results are consistent with disturbed osteogenesis and osteoclastogenesis in various growth sites of the skull (sutures, growth centers of membranous ossification, growth cartilage of endochondral ossification and periosteal areas) in response to *Msx2* deficiency, as observed in previous studies on the role of *Msx2* in bone modeling (9, 14). The functional role of *Msx2* was investigated in *in vitro* cell culture assays and was found to be related to the osteogenic commitment of pluripotent cells (15, 16), the stimulation of osteoblast precursors proliferation (14), and the prevention of osteoblast terminal differentiation (17).

Cephalometric analysis of the craniofacial skeleton, as performed in the present study, additionally permitted defining precisely the anatomical bone sites where *Msx2* expression plays a decisive role. This is advantageous compared with whole mount staining techniques where the expression of a gene at a specific site is shown but without determining its real contribution in the resulting anatomy.

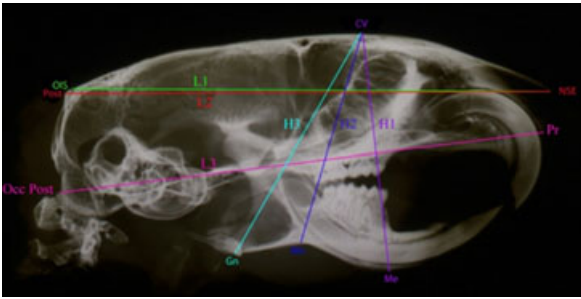


Fig. 3. Craniofacial length and height (*Msx2*<sup>+/+</sup>).

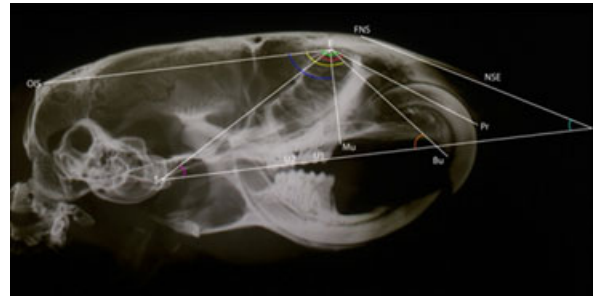


Fig. 7. Viscerocranium angles (*Msx2*<sup>+/+</sup>).

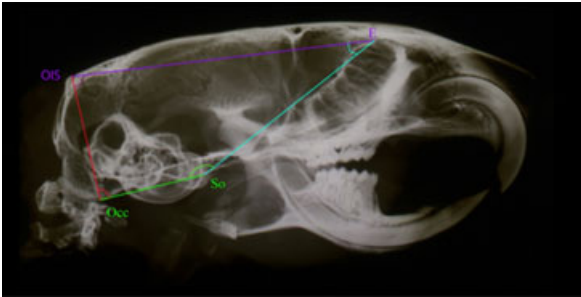


Fig. 4. Neurocranium distances and angles (*Msx2*<sup>+/+</sup>).

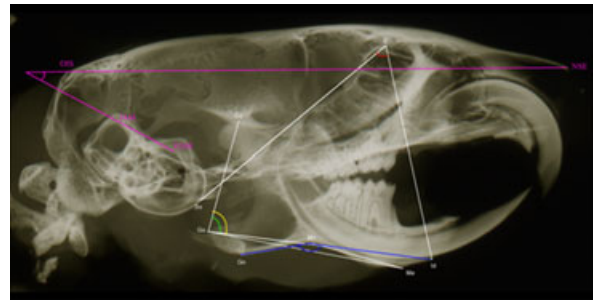


Fig. 8. Mandible and cochlear apparatus angles (*Msx2*<sup>+/-</sup>).

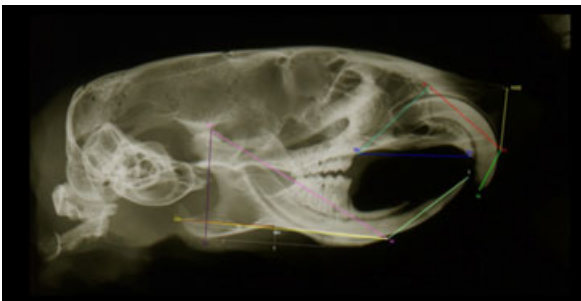


Fig. 5. Viscerocranium and mandible distances (*Msx2*<sup>+/-</sup>).

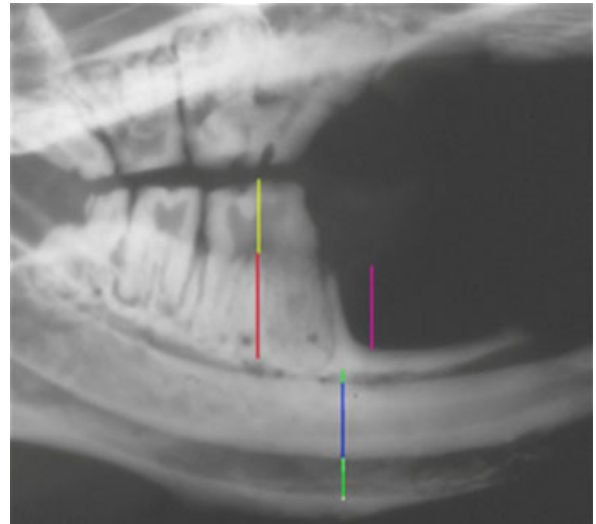


Fig. 9. Dento-alveolar complex (*Msx2*<sup>-/-</sup>).



Fig. 6. Bases and arches discrepancies (*Msx2*<sup>+/+</sup>).

**The *Msx2*<sup>+/-</sup> mice present a specific phenotype**

In addition to these findings in the *Msx2* null mice, this analysis also reported a specific phenotype in the *Msx2* heterozygous mice, whereas



Fig. 10. Incisor's curvature (*Msx2*<sup>-/-</sup>).

previous studies stated that the *Msx2*<sup>+/-</sup> mice were undistinguishable from the wild-type mice (8, 9). Analysis of the recorded measurements showed that many cephalometric values, such as the neurocranium shape (Occ-OIS/Occ-So, So-Occ/So-E), the anterior facial height (NSE-Pr), the central viscerocranium height (E-Mu), the palatal length (Mu-Bu), the mandibular ramus length, the thickness of the lingual periodontal ligament, and the anatomical crown height of the lower first molar were significantly different between the *Msx2* heterozygous and the wild-type mice.

Surprisingly, on four sites, the *Msx2*<sup>+/-</sup> phenotype revealed to be not intermediate between the *Msx2*<sup>-/-</sup> and the *Msx2*<sup>+/+</sup> animals. Actually, the postero-inferior angle of the neurocranium (Occ-OIS/Occ-So) was increased in the *Msx2*<sup>-/-</sup> animals, while it was decreased in the heterozygous mice. The skull base angle (So-Occ/So-E), the central height of the viscerocranium (E-Mu), and the mandibular ramus length (Go-Mn) were decreased in the *Msx2*<sup>-/-</sup> mice, while they were increased in the *Msx2*<sup>+/-</sup> mutant mice. In addition, the use of a quantitative analysis on electron microscope of the *Msx2* mutant mice enamel thickness allowed Molla et al. (18) to show that the *Msx2*<sup>+/-</sup> mice presented an increased thickness of the enamel layer compared with the wild-type mice, whereas the *Msx2*<sup>-/-</sup> mice showed a very reduced enamel tissue. Therefore, the *Msx2*<sup>+/-</sup> phenotype is not intermediate between the *Msx2*<sup>-/-</sup> and the *Msx2*<sup>+/+</sup> ones. The phenotypic effects of *Msx2* haploinsufficiency in cranial morphology point to a nonlinear effect of *Msx2* gene dosage in craniofacial development. Collectively, these results underline an *Msx2* site-specific activity which could be noted only with quantitative measurements as cephalometric analysis. Such technique should be associated in the future to any phenotype characterization. In others words, when a phenotype in relation with a gene mutation is described, the morphological modifications should be quantified to appreciate the activity of the modified gene in each bone and even in each part of the bones.

#### ***Msx2* involvement in neurocranium and viscerocranium shape and size**

In this study, the neurocranium of the *Msx2*<sup>-/-</sup> mice was reduced with concomitant alteration of its shape. These results agree with previous reports observed in *MSX2* human mutations, showing (1) enlarged parietal foramina in loss-of-function of *MSX2* mutation (7) and (2) craniosynostosis Boston type in gain-of-function of *MSX2* mutation (6). The growth pattern of the neurocranium is closely related to the enlargement of the brain (19, 20). Thus, the *Msx2*<sup>-/-</sup> mice craniofacial dysmorphies could cause important constraints limiting brain development. This hypothesis could also explain the generalized seizure-like episodes previously reported in these mutant mice (8). Alternatively, this cephalometric study pointed out a dysmorphism of the cochlear apparatus, which can be responsible for the loss of balance observed in the *Msx2*<sup>-/-</sup> mutant animals. If it is confirmed, in presence of unexplained loss of balance in human clinic, *Msx2* mutations investigations should be undertaken.

*Msx2*<sup>-/-</sup> mice viscerocranium size and shape were modified. We recorded a maxilla retrusion (E-Pr/E-So, E-Pr/E-OIS) in the *Msx2*<sup>-/-</sup> mice which might be directly related to a maxilla size reduction. Indirectly, the retrusion of the maxilla and the hypodeveloped cranio-facial skeleton in the *Msx2*<sup>-/-</sup> mice could be correlated to a reduced masticatory function caused by the amelogenesis imperfecta present in these animals. This reduced masticatory function would be a key determinant for the hypodevelopment of the facial skeleton in these mice as underlined by Kiliaridis et al. (12) in rats. Furthermore, the observed increase in anterior facial length (NSE-Pr) in the *Msx2*<sup>-/-</sup> mice and to a lesser extent in the *Msx2*<sup>+/-</sup> mice, compared with the wild type, might be related to the observed reduced curvature of the upper incisor of the mutant animals. In mice, the upper incisor occupies almost the totality of the upper viscerocranium. The present study could not determine whether the modifications of the shape of the upper viscerocranium

are the result or cause of the modifications of the shape of the upper incisors.

Finally, the shape of the mandible was only slightly modified because the angular process length (Go-Mn) was smaller and the gonial angle (Go-Co/Go-Me) was larger. The latter open-bite sign of the mandibular morphology could also be explained by a decrease in the masticatory function of these animals.

#### **Msx2 and alveolodental complex development**

Satokata et al. (8) showed that the *Msx2*<sup>-/-</sup> knock-out mice displayed a wide spectrum of alterations of the teeth, ranging from eruption to morphology abnormalities and periodontal defects (8). These mutant mice exhibited a reduced and irregular enamel, dentin, cementum, and periodontal ligament thickness in molars and incisors (9). This study confirmed these previous results. The reduced size of the upper and lower incisor observed in the *Msx2*<sup>-/-</sup> mice is related to an excessive crown abrasion due to amelogenesis imperfecta. The increased thickness of the incisors' buccal periodontal ligament and the overall reduced thickness of the incisors observed in the *Msx2*<sup>-/-</sup> mice confirm also the lack of enamel production related to the amelogenesis imperfecta. Enamel deficiency could finally be responsible for the reduced internal and external curvature of the upper and lower incisors in the *Msx2*<sup>-/-</sup> mice. This reduced curvature could be also related to the modified shape and size of the maxillary and the mandible where the incisors develop. Thus, unexplained amelogenesis imperfect could be related to a potential *Msx2* mutation. The reduced thickness of the lingual periodontal ligament of the lower incisor teeth is in accordance with Yoshisawa et al. (21) who showed *in vitro* that *Msx2* overexpression down-regulated the osteoblast terminal differentiation and the mineralization of the extracellular matrix. *Msx2* would have a preventing role in the ossification of the periodontal ligament. So, unexplained ankylosis could be related to *Msx2* mutations.

A significant reduction in the vertical dimension of the lower first molar was observed in the *Msx2*<sup>-/-</sup> mice compared with the two other

groups. The root height was strongly reduced. Furthermore, the pulp floor and the tooth furcation were dislocated in the apical direction, and the pulp height was increased in the *Msx2*<sup>-/-</sup> and in the *Msx2*<sup>+/-</sup> mice. Thus, these mutant mice display the characteristics of taurodontism. This is consistent with the observations of Yamashiro et al. (22) who found a high concentration of *Msx2* in the dental pulp of 14 days-old mice. *Msx2* deficiency could prevent the differentiation of the odontoblasts, thereby explaining the smaller dentin thickness and the larger pulp cavity in the *Msx2*<sup>-/-</sup> mice. Taurodontism is caused by a failure of Hertwig's epithelial root sheath diaphragm to invaginate at the proper horizontal level (23, 24). This finding is consistent with the results of Aioub et al. (9) who showed that the *Msx2*<sup>-/-</sup> mice presented important morphological anomalies of the Hertwig Epithelial Root Sheath. Jaspers and Witkop (25) have noticed that severe forms of taurodontism were associated with X chromosomal aneuploidy. Taurodontism is also associated with hypohidrotic ectodermal dysplasia (HED) caused by mutations of genes involved in the ectodysplasin NF- $\kappa$ B (EDA) pathway: *EDA*, *EDAR*, *NEMO* genes. This dysmorphology is likewise related to the tricho-dento-osseous (TDO) syndrome in relation with *DLX3* mutation. So taurodontism could be one of the symptomatic signs of *Msx2* mutations.

The next steps of this research will be the use of 3D CT scan data: first 'in vitro' for its accuracy and then 'in vivo' to explore growth dynamics. 3D data will allow the exploration of the transversal dimension and will suppress superimpositions, making the location of the different landmarks more accurate. The application of geometric morphometrics (shape analyses) on this sample of radiographs (2D) and then on 3D data will provide more information about the implication of *Msx2* in the craniofacial growth.

## **Conclusion**

Cephalometric analysis applied on profile micro-radiographs of mutant animals is revealed to be a

very powerful tool to precisely record and quantify bone abnormalities induced by gene mutation. In the current setting of *Msx2* mutation, the cephalometric analysis points out the role of *Msx2* on the different components of the craniofacial growth pattern. *Msx2* seems to have a preventing role in premature ossification of the craniofacial growth sites as well as of the periodontal ligament, explaining therefore the reduced size of the craniofacial bones and the reduced thickness of the lingual periodontal ligament in the *Msx2*<sup>-/-</sup> mice. This cephalometric analysis enabled recording substantial differences in the craniofacial morphology of the *Msx2*<sup>+/-</sup> mice, demonstrating a specific phenotype which was not reported previously. This phenotype was not intermediate between the *Msx2*<sup>-/-</sup> and the wild-type mice. In conclusion, all these morphological parameters previously described, namely a modified height of the posterior part of the skull, a rotated cochlear apparatus, enamel structure anomalies, a taurodontism, could be symptomatic signs of a *Msx2* mutation.

## Clinical relevance

*MSX2* is implicated in two human pathologies that provoke defaults in craniofacial sutures. Furthermore, *Msx2* is involved in bone physiology and in tooth morphogenesis. The prognosis for treatment outcome in orthodontics depends on craniofacial growth. However, few data on genetic etiology of craniofacial growth are available. This study screens the dysmorphologies associated with loss-of-function mutation of *Msx2* allowing a better insight of the role of this gene in craniofacial morphology and growth. In addition, this study provides morphological signs such as a rotated cochlear apparatus, enamel structure anomalies, and taurodontism which could be symptomatic of an *Msx2* mutation.

**Acknowledgments:** We thank Benoit ROBERT (Pasteur Institute) for providing us the *Msx2* mutant mice and ANR Osteodiversity funding for its financial support.

## References

- Francis-West PH, Robson L, Evans DJR. *Craniofacial Development: The Tissue and Molecular Interactions that Control Development of the Head*. Berlin: Springer Press; 2003.
- Alappat S, Zhang ZY, Chen YP. *Msx* homeobox gene family and craniofacial development. *Cell Res* 2003;13:429–42.
- MacKenzie A, Ferguson MW, Sharpe PT. Expression patterns of the homeobox gene, *Hox-8*, in the mouse embryo suggest a role in specifying tooth initiation and shape. *Development* 1992;115:403–20.
- Berdal A, Molla M, Hotton D, Aioub M, Lezot F, Nefussi JR et al. Differential impact of *MSX1* and *MSX2* homeogenes on mouse maxillofacial skeleton. *Cells Tissues Organs* 2009;189:126–32.
- Orestes-Cardoso S, Nefussi JR, Lezot F, Oboeuf M, Pereira M, Mesbah M et al. *Msx1* is a regulator of bone formation during development and postnatal growth: in vivo investigations in a transgenic mouse model. *Connect Tissue Res* 2002;43:153–60.
- Jabs EW, Müller U, Li X, Ma L, Luo W, Haworth IS et al. A mutation in the homeodomain of the human *MSX2* gene in a family affected with autosomal dominant craniosynostosis. *Cell* 1993;75:443–50.
- Wilkie AO, Tang Z, Elanko N. Functional haploinsufficiency of the human homeobox gene *Msx2* causes defects in skull ossification. *Nat Genet* 2000;24:387–90.
- Satokata I, Ma L, Ohshima H. *Msx2* deficiency in mice causes pleiotropic defects in bone growth and ectodermal organ formation. *Nat Genet* 2000;24:391–5.
- Aioub M, Lézot F, Molla M, Castaneda B, Robert B, Goubin G et al. *Msx2*<sup>-/-</sup> transgenic mice develop compound amelogenesis imperfecta, dentinogenesis imperfecta and periodontal osteopetrosis. *Bone* 2007;41:851–9.
- Engstrom C, Linde A, Thilander B. Craniofacial morphology and growth in the rat. Cephalometric analysis of the effects of a low calcium and vitamin D-deficient diet. *J Anat* 1982;134:299–314.
- Lallemand Y, Nicola M-A, Ramos C, Bach A, Cloment CS, Robert B. Analysis of *Msx1*; *Msx2* double mutants reveals multiple roles for *Msx* genes in limb development. *Development* 2005;132:3003–14.
- Kiliaridis S, Engstrom C, Thilander B. The relationship between masticatory function and craniofacial morphology. I. A cephalometric longitudinal analysis in the growing rat fed a soft diet. *Eur J Orthod* 1985;7:273–83.
- R-Development-Core-Team. *R: A Language and Environment for Statistical Computing*. Vienna, Austria: R Foundation for Statistical Computing; 2011.
- Cheng SL, Shao JS, Cai J, Sierra OL, Towler DA. *Msx2* exerts bone anabolism via canonical Wnt signaling. *J Biol Chem* 2008;283:20505–22.
- Ichida F, Nishimura R, Hata K, Matsubara T, Ikeda F, Hisada K et al. Reciprocal roles of *Msx2* in regulation of osteoblast and adipocyte differentiation. *J Biol Chem* 2004;279:34015–22.

16. Cheng S-L, Shao J-S, Charlton-Kachigian N, Loewy AP, Towler DA. Msx2 promotes osteogenesis and suppresses adipogenic differentiation of multipotent mesenchymal progenitors. *J Biol Chem* 2003;278:45969–77.
17. Dodig M, Tadic T, Kronenberg MS. Ectopic Msx2 overexpression inhibits and Msx2 antisense stimulates calvarial osteoblast differentiation. *Dev Biol* 1999;209:298–307.
18. Molla M, Descroix V, Aioub M, Simon S, Castaneda B, Hotton D et al. Enamel protein regulation and dental and periodontal physiopathology in MSX2 mutant mice. *Am J Pathol* 2010;177:2516–26.
19. Hoyte DAN. Mechanisms of growth in the cranial vault and base. *J Dent Res* 1971;50:1447–61.
20. Cohen MM Jr. Sutural biology and the correlates of craniosynostosis. *Am J Med Genet* 1993;47:581–616.
21. Yoshizawa T, Takizawa F, Iizawa F, Ishibashi O, Kawashima H, Matsuda A et al. Homeobox protein Msx2 acts as a molecular defense mechanism for preventing ossification in ligament fibroblasts. *Mol Cell Biol* 2004;24:3460–72.
22. Yamashiro T, Tummers M, Thesleff I. Expression of bone morphogenetic proteins and Msx genes during root formation. *J Dent Res* 2003;82:172–6.
23. Jafarzadeh H, Azarpazhooh A, Mayhall JT. Taurodontism: a review of the condition and endodontic treatment challenges. *Int Endod J* 2008;41:375–88.
24. Terezhalmay GT, Riley CK, Moore WS. Clinical images in oral medicine and maxillofacial radiology. Taurodontism. *Quintessence Int* 2001;32:254–5.
25. Jaspers MT, Witkop CJ Jr. Taurodontism, an isolated trait associated with syndromes and X-chromosomal aneuploidy. *Am J Hum Genet* 1980;32:396–413.

Copyright of Orthodontics & Craniofacial Research is the property of Wiley-Blackwell and its content may not be copied or emailed to multiple sites or posted to a listserv without the copyright holder's express written permission. However, users may print, download, or email articles for individual use.